

# Biologically Inspired Compliant Control of a Monopod Designed for Highly Dynamic Applications

Sebastian Blank, Thomas Wahl, Tobias Luksch, and Karsten Berns

**Abstract**—In this paper the compliant low level control of a biologically inspired control architecture suited for bipedal dynamic walking robots is presented. It consists of elastic mechanics, a low-level compliant joint controller and a hierarchical reflex-based control layer. The former is implemented on a DSP while the reflex network is located on a desktop PC. Thus, one is able to utilize distribution as a powerful means to guarantee low latency and scalability.

The concept is tested on a prototype leg mounted on a vertical slider that is designed to perform cyclic squat jumps. Thus, a suited mechatronic setup that features highly dynamic actuators as well as energy storage capabilities is derived. Cyclical jumping is employed as a benchmark for the system's performance. Experimental results of the prototype setup as well as simulation runs are presented and compared to human squat jumping.

## I. INTRODUCTION

A feature that has proven to be amongst the most challenging to recreate in the field of robotics is the human ability of biped locomotion. This is mainly caused by the fact that walking, running, or jumping are highly complex processes. In order to achieve the long term goal of designing a walking machine with superior properties, several problems have to be dealt with on the way. First of all it involves the need for energy efficient actuation, sophisticated control architectures and algorithms, and an elaborate mechanical design. At the same time it is posing restrictions concerning stability and weight as well as limiting the amount of data bandwidth to be used in the process.

Therefore, a concept will be presented in this paper transferring these aspects from natural motion control to a technical system on several levels. The key features are a non-retardant actuation concept, high energy efficiency through the introduction of elastic elements into the mechanical setup, inherent robustness, and a control concept that is highly scalable concerning the introduction of additional DOF in the design process. The approach taken utilizes the reactive control paradigm in form of a network including higher level skills and low-level reflexes as well as physical distribution between a central processing unit and several DSPs in the proximity of the actuators. The key features to be realized are natural motions and the already mentioned high energy efficiency. The former is achieved through compliant control of DC actuators while the latter can be realized by allowing the system inherent natural dynamics to unfold.

Sebastian Blank, Thomas Wahl, Tobias Luksch, and Karsten Berns are with the Robotics Research Lab, Department of Computer Sciences, University of Kaiserslautern, PO Box 3049, 67663 Kaiserslautern, Germany {blank}, {wahl}, {luksch}, {berns}@cs.uni-kl.de

## II. RELATED WORK

Compliant actuation is considered to be the key element in locomotion approaches featuring natural motions, good energy efficiency, and robustness. This statement is mainly supported by the compliance of the muscle-tendon system that can be shown to play an essential role during biological locomotion. Furthermore, compliance can help to reduce the potential damage to objects or persons within the area of operation.

None of the actuators developed so far can live up to their biological archetypes, whose power to weight ratio and dynamical properties have yet to be reached. Nevertheless, they represent means to achieve a system behavior that is roughly comparable to that of a natural system. Compliant actuation approaches can be categorized into two groups: those that realize compliance by means of mechanical design and the other group that utilizes software-based control approaches.

For the group of hardware-based approaches there exist countless examples. Very typical candidates from this group are MACCEPA [1], series elastic actuators [4], VIA [2], fluidic muscles, and the AMASC [3] approach. Although their properties are very interesting, each approach shows distinct drawbacks. For instance, some of the designs display very high complexity or significant weight. Also, energy efficiency is limited due to e.g. increased friction caused by more moving parts. Further restrictions are introduced by the properties of available component (e.g. spring stiffness).

Similarly, some disadvantages can be identified within the second group. Typical examples of the software-based approaches to achieve compliance are impedance control [5], computed torque method [6], and virtual model control [7], [8]. Their main common drawback is the necessity for high system bandwidth and additional sensors. The former causes them to be not suitable for the approach taken in this paper since the desired field of application is highly dynamic.

Accordingly, two kinds of compliance can be distinguished: active and passive. Active compliance is achieved by making use of force-based feedback control. If, for example, a robotic manipulator collides with an obstacle active compliance enables it to deliberately retreat while passive compliance only limits the force applied. The latter is usually realized using mechanically compliant components. Since both have their distinct advantages we attempt to realize both by combining springs (passive) with an active torque control structure.



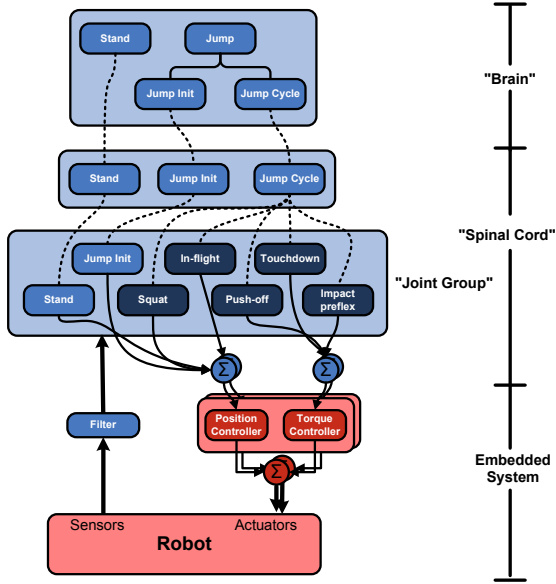


Fig. 2. Schematic overview of the behavior network controlling the motion of the jumping leg

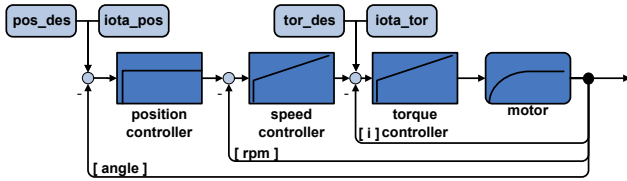


Fig. 3. Threefold cascaded actuator control structure

springs are attached to the knee joint to store energy in the squat phase.

Biological joints are actuated by an antagonistic layout of two muscles. According to the physiologist A. Hill, the muscles can be described as a contracting actuator combined with serial and parallel springs and damping (see [11], p. 78).

The non-linear behavior of the serial springs in the antagonistic setup allows the adjustment of the stiffness. A biologically joint-like behavior implies the existence of adjustable compliance. This is implemented using a low-level controller that is comprised of a threefold cascaded structure. A schematic layout of the controller and its interface is presented in figure 3. To ensure real-time performance and a low delay the controller is implemented on a DSP with a cycle time of 1 ms. The inner control loop is constructed as a torque controller. The controller adjusts the actual motor current measured by the DSP. The measurement is synchronized with the 39 kHz-PWM. This setup did prove to be fast enough to realize an average torque rise time of 8 ms.

The input ( $current_{des}$ ) for the torque controller is the fusion of the desired torque ( $tor_{des}$ ) and the output of the speed controller ( $tor_{speed}$ ). These inputs are weighted by

two values  $l_{pos}, l_{tor} \in [0, 1]$  (see equation 1).

$$current_{des} = \frac{l_{pos} \cdot (l_{pos} \cdot tor_{speed}) + l_{tor} \cdot (l_{tor} \cdot tor_{des})}{l_{pos} + l_{tor}} \quad (1)$$

This weighted sum allows the adjustment of the joint stiffness. With rising  $l_{pos}$  from zero to one and decreasing  $l_{tor}$  from one to zero the behavior changes from a compliant torque controlled joint to a completely stiff joint. The weights are normalized to the range between zero and one.

The speed controller solely acts as a slave controller for the position controller. The former possesses no direct input from the higher behaviors as it is not required by the reflex network. Due to the integral portion of the system the position controller has no need for an integral part. To ensure stability, several low pass filters and limiters are introduced in between the different controllers.

In order to determine the optimum controller gains the respective transfer functions have to be derived as suggested in [19]. It is advised to start with the inner most control loop: the torque (current) controller. Its open loop transfer function can be denoted as:

$$G_0(s) = k_{Pi} \cdot \frac{1 + s \cdot T_{Di}}{s \cdot T_{Di}} \cdot \frac{1}{1 + s \cdot T_{\sigma}} \cdot \frac{K_A}{1 + s \cdot T_A} \quad (2)$$

Here,  $k_{Pi}$  and  $T_{Di}$  are the gain and time constant of the PI torque controller. The middle section of the equation represents a smoothing element in the feedback loop with the time constant  $T_{\sigma}$ . The last fraction is a PT1 model of the motor with gain  $K_A$  and time constant  $T_A = \frac{L_A}{R_A}$ . Approximating the time constant  $T_{Di}$  with the electrical armature constant  $T_A$  and trying to achieve a steady gain over the spectrum yields a gain of  $k_{Pi} = \frac{T_A}{2T_{\sigma}K_A}$ . These constraints lead to the simplified closed loop transfer function given in equation 3.

$$G(s) = \frac{1}{1 + s \cdot 2T_{\sigma} + s^2 \cdot 2T_{\sigma}^2} \quad (3)$$

Due to the damping characteristics the controller/plant can be simplified to a PT1 element with a combined time constant  $T_S$ . The inertia of the motor is represented by  $T_{idle}$ . Combining these elements with the speed controller leads to the transfer function of the open loop as denoted in equation 4.

$$G_{0n}(s) = k_{Pn} \cdot \frac{1 + s \cdot T_{Dn}}{s \cdot T_{Dn}} \cdot \frac{1}{1 + s \cdot T_S} \cdot \frac{1}{s \cdot T_{idle}} \quad (4)$$

To maximize the phase margin and thus increase stability, the time constant  $T_{Dn}$  is set to the 'symmetric optimum'  $T_{Dn} = 4T_S$  and the gain to  $k_{Pn} = \frac{T_{idle}}{\sqrt{T_{Dn}T_S}}$ . The result of these simplifications is a closed loop transfer function of the cascaded controller that is solely dependent on one free parameter  $T_S$ . The order of the system can therefore be reduced from five to three and can be investigated with common formal methods.

$$G_n(s) = \frac{1 + s \cdot T_{Dn}}{1 + s \cdot T_{Dn} + s^2 \cdot \frac{T_{Dn}T_{idle}}{k_{Pn}} + s^3 \cdot \frac{T_{Dn}T_{idle}T_S}{k_{Pn}}} \quad (5)$$

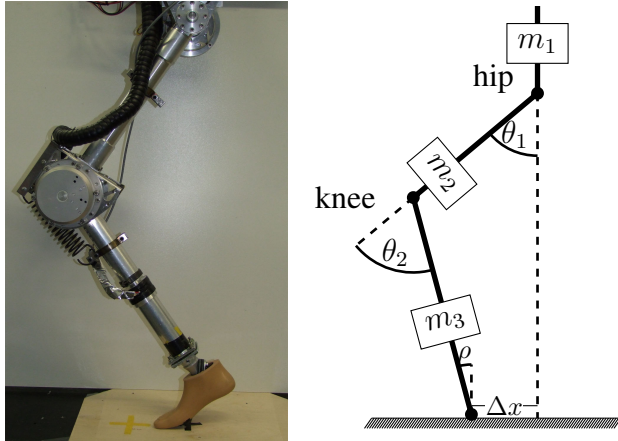
$$\frac{T_{Dn} \cdot k_{Pn}}{1 + s \cdot 4T_S + s^2 \cdot 8T_S^2 + s^3 \cdot 8T_S^3} \quad (6)$$

### C. Distributed Concept

The presented compliant control approach allows the distribution of reflexes and skills onto different processing units (PU). For the experimental setup two different PUs are used. For the latency critical reflexes DSP-nodes were employed: These nodes consist of a DSP combined with a CPLD. The reflexes and skills with lower timing demands are processed on a standard PC. All DSP-nodes are connected via CAN bus to the PC. There are no real-time properties required, since the time critical sensor information is utilized only locally within one node. All the other information that is required in the higher-level behaviors is preprocessed in the DSPs. Local and simple reflexes allow the encapsulation on one DSP. This distributed control approach makes the system highly scalable, because in case additional sensors or actuators are required the respective nodes can easily be integrated into the CAN bus structure. Due to the fact that all reflexes are distributed on several nodes, the system is robust to disturbances or hardware malfunction of single PUs or the CAN bus. Another benefit from the distributed concept is reduced wiring effort and lower noise level.

## IV. EXPERIMENTAL VALIDATION

In order to test the previously described approach the single leg was modeled within a dynamical simulation framework to simulate the real leg behavior. The dimensions, segment weights and the motor and spring characteristics of the real prototype leg were used to achieve realistic results.



(a) Prototype leg mounted a vertical slider (b) Graphic representation of the leg model suited for the simulation

Fig. 4. Prototype leg and the simulation model

The leg prototype is shown in figure 4(a) while the simulation model is displayed in figure 4(b). The leg is mounted on a vertical slider above the hip joint that only allows for up-and-down movement. Besides the slider it possesses two rotational DOF at the hip and knee joint that are both actuated. Besides the DC motors with a low ratio gear of 1 : 32 that is needed to be non-retardant, a linear spring is installed in parallel to the knee. It serves as energy storage during the cyclic motion in order to be

able to preserve the otherwise lost impact energy. The foot is implemented by a commercial CFRP prosthesis.

The overall length of the system from foot to hip is 0.97 m and the overall weight is approx. 15.5 kg. The setup is equipped with angle encoders at either joint, a load cell mounted in the lower limb and current probes at both actuators.

### A. Disturbance Compensation

In order to show the robustness of the approach taken, the first experiment (figure 5) demonstrates the system behavior in response to external disturbances. For this purpose the ground level (top) was altered several times in the simulation environment while the leg was in the air to simulate obstacles such as stairs. The respective system reaction is depicted in the three graphs below. They display (from top to bottom) the height level of the torso, the knee angle, and the force in z-direction recorded via the load cell in the lower limb. Six jump cycles are shown.

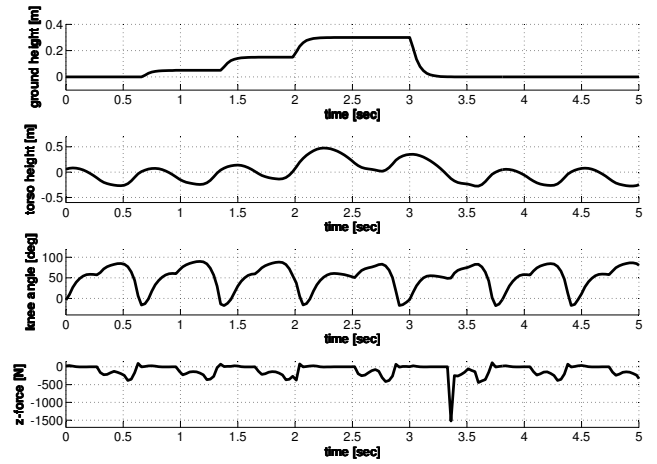


Fig. 5. Data gathered during a series of disturbed jump cycles

As one can see even a very severe distortion (30 cm ground level shift during the 5th jump cycle at  $t \approx 3.4$  sec) is not able to interrupt the continuity of the motion. This indicates that for the given restrictions the demanded robustness is actually achieved in the implemented system.

### B. Comparison to Human Squat Jump

After the cyclic squat jump could be realized using the simulation with a peak jump amplitude of approx. 14 cm above the fully extended position, the similarity of the simulated data with human squat jump trajectories is investigated. In figure 6 the hip and knee angles are presented for a full jump cycle.

A full jump cycle can be roughly divided into three phases: push-off, phase without ground contact, and the impact. The recorded jump cycle begins at the lowest position that is reached after the preceding touchdown phase. Thus, the first action that is induced by the behavior network is to extend the leg in order to reach a speed that is sufficient to leave the ground (0–35%). During the airborne phase (35–70%) the

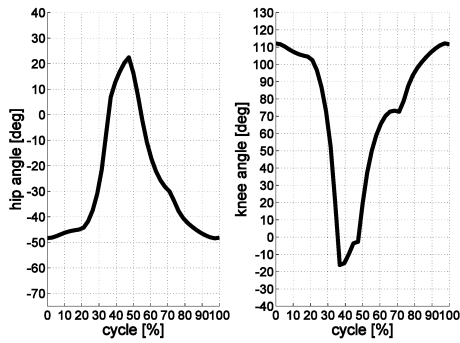


Fig. 6. Angular trajectory of hip and knee joint based on data acquired during simulated squat jump

leg is retracted and brought into a safe landing position. The subsequent impact phase is used to compensate the surplus energy (that is partly stored in the parallel spring) and bring the leg in a controlled resting position that marks the end of the cycle. It is to be pointed out that the trajectory of the simulated leg is not designed to look like a human one but is rather the result of the interaction of the behavior network that is used to control it.

It is reasonable to assume a human trajectory when looking for a benchmark since it is highly optimized with respect to energy efficiency and robustness. Thus, motion capture was performed on five different subjects to acquire the data that serves as means of comparison. Optical markers were placed at the hip, knee, and foot. Their respective location was tracked with a sample frequency of 250 Hz. The data of two subjects is presented in figures 7 and 8.

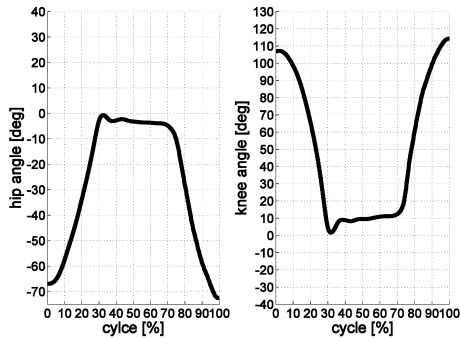


Fig. 7. Data gathered using motion capture on a human subject performing a squat jump

Comparing the human to the leg prototype motion, significantly longer flight phase of the human subjects can be observed. This is caused by the tremendously higher efficiency of muscles compared to the used DC motors. Thus, a higher lift-off velocity can be achieved resulting in a higher peak amplitude. The second difference is the distinct pre-flexion that occurs in the simulated leg but not in the natural trajectory. This is the case as human anatomy (i.e. the existence of the Achilles' tendon) makes a distinct pre-bending mostly obsolete.

Besides these differences, the simulated data closely re-

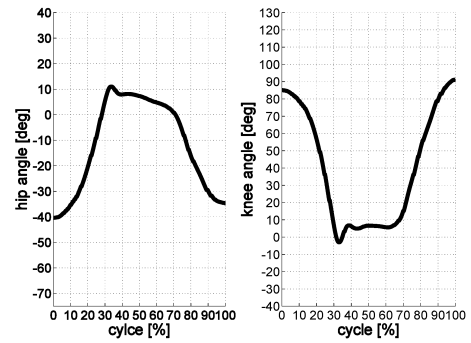


Fig. 8. Graph depicting the angular trajectory of a second subject performing the same jump pattern

sembles the human role model. The angular range is about equal as well a certain details such as the peak in the knee angle (simulation at approx. 38 %, human data approx. 30 %). Therefore, it can be stated that an approximately equal characteristics like the biological role model could be realized with the behavior network.

### C. Impact Behavior

The next step is to transfer the simulation results on the physical prototype leg setup. As a first step towards this task, the influence of the compliance setting was determined in a preliminary experiment. It is intended to serve as a means to demonstrate the capabilities of the proposed joint controller. For this purpose the leg was manually lifted to an amplitude of approx. 10 cm above initial stretched out position. Since the leg is flexed (hip angle  $\approx 30^\circ$ , knee angle  $\approx 58^\circ$ ) the resulting drop height is approx. 30 cm. The leg is then released using different joint compliance setting for the knee while relaxing the hip joint. Three resulting angle trajectories for a compliant, intermediate, and stiff setup are presented in figure 9.

It can be seen that the compliance influences both the amplitude and the duration of the disturbance that is caused by the impact. As expected the length of the disturbed interval decreases with increasing stiffness by about 42 %. In the same manner the amplitude decreases by more than 60 %. The first drop with the compliant setup is not completely comparable with the others, because the initial position is not the same. This is the result of the compliant position controller and the parallel spring. The spring tries to extend the knee. After the impact the weight of the upper part counteracts the spring tension.

## V. CONCLUSIONS AND OUTLOOK

### A. Conclusions

In this paper a behavior network and low-level compliant control approach were introduced. The distributed system including a standard desktop PC and several DSP PUs was implemented and a prototype leg was built in order to verify the data acquired during the simulation process on a physical system. The simulation results were verified using data gathered during a motion capture of several human

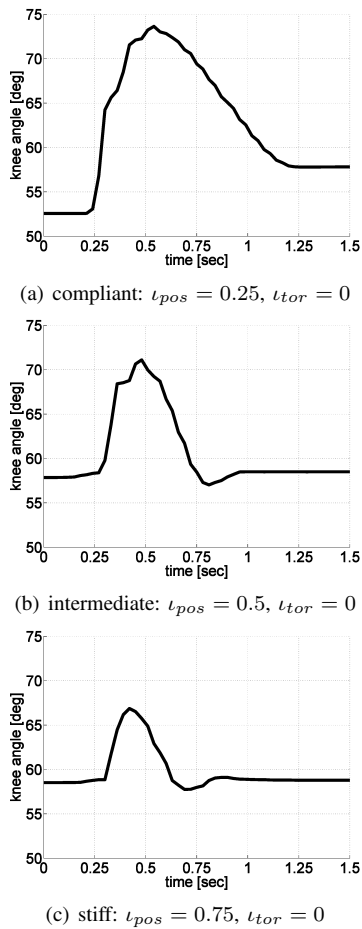


Fig. 9. Impact experiment performed with the mechanical foot setup

subjects. They served as a biological benchmark for the system performance.

Preliminary experiments on the physical prototype leg were performed. The focus of this first stage of experiments was the influence of the compliant capabilities on the physical behavior of the leg in a highly dynamic situation.

The results acquired during the experiments have shown the potential of the system. It underlines that it is well suited for natural-looking, energy efficient, and robust motion in the context of highly dynamic application. Furthermore, the need for compliance is emphasized by the presented results.

### B. Future Works

The next step in the system development is performing the entire adaption to the prototype leg. Thus, one will be able to perform cyclical squat jumps under the given restrictions.

In order to enhance the performance it seems reasonable to adapt the passive foot construction to the dynamic setup. Therefore, rather than using a commercially developed foot prosthesis, a CFRP construction that is especially adapted to the application scenario an prototype characteristics should be designed and built.

An inertial system will be added to the setup as well. This allows to obtain more information about the center of gravity and thus increase the system performance.

Once the jump can be performed with the setup successfully, the next step should be to gradually increase the degree of freedom of the hip. As a first step a second horizontal slider can be employed while later on adding a rotational DOF as well. Thus, one will be able to receive more realistic data from the experimental setup.

### REFERENCES

- [1] R. Van Ham, B. Vanderborgh, M. Van Damme, B. Verrelst, D. Lefeber, "MACCEPA, the mechanically adjustable compliance and controllable equilibrium position actuator: Design and implementation in a biped robot", *Robotics and Autonomous Systems*, vol. 55, no. 10, January 2007.
- [2] G. Tonietti, R. Schiavi, A. Bicchi, "Design and Control of a Variable Stiffness Actuator for Safe and Fast Physical Human/Robot Interaction", in *IEEE International Conference on Robotics and Automation*, Barcelona, Spain, 2005, pp. 528-533.
- [3] J.W. Hurst, A.A. Rizzi, "Series Compliance for an Efficient Running Gait: Lessons Learned from the Electric Cable Differential Leg", in *IEEE Robotics and Automation Magazine*, vol. 15, no. 3, September 2008, pp. 42-51.
- [4] G.A. Pratt, M.M. Williamson, "Series Elastic Actuators", in *Proceedings of the IEEE/RSJ International Conference on Intelligent Robots and Systems*, Pittsburgh, USA, 1995, pp. 399-406.
- [5] J.H. Park, "Impedance Control for Biped Robot Locomotion", in *IEEE Transactions on Robotics and Automation*, vol. 17, no.6, December 2001
- [6] K. Loeffler, M. Gienger, F. Pfeiffer, H. Ulbrich, "Sensors and Control Concept of a Biped Robot", in *IEEE Transactions on Industrial Electronics*, vol. 51, no. 5, October 2004, pp. 972-980.
- [7] J. Pratt, C.M. Chew, A. Torres, P. Dilworth, G. Pratt, "Virtual Model Control: An Intuitive Approach for Bipedal Locomotion", in *International Journal of Robotics Research*, vol. 20, no. 2, 2001, pp. 129-143
- [8] T. Kerscher, M. Goeller, J. M. Zoellner, R. Dillmann, "Regelungsstrategie fuer Zweibeiniges Elastisches Laufen Mittels 'Virtual Model Control'", in *Autonome Mobile Systeme*, Kaiserslautern, Germany, 2007, pp. 268-274
- [9] M. A. Lemay, J. E. Galagan, N. Hogan, E. Bizzi, "Modulation and vectorial summation of the spinalized frog's hindlimb end-point force produced by intraspinal electrical stimulation of the cord", *IEEE Transactions on Neural Systems and Rehabilitation Engineering*, vol. 9, March 2001.
- [10] E. Bizzi, V. Cheung, A. d'Avella, P. Saltiel, M. Tresch, "Combining modules for movement", *Brain Research Reviews*, vol. 57, pp. 125-133, 2007.
- [11] J. Hamill, K.M. Knutzen, "Biomechanical Basis of Human Movement", *Lippincott Williams & Wilkins*, 2nd ed., 2003.
- [12] Y. P. Ivanenko, R. E. Poppele, F. Lacquaniti, "Five basic muscle activation patterns account for muscle activity during human locomotion", *Journal of Physiology*, vol. 556, 2004.
- [13] Y. P. Ivanenko, R. E. Poppele, F. Lacquaniti, "Motor Control Programs and Walking", *The Neuroscientist*, vol. 12, no. 4, pp. 339-348, 2006.
- [14] E. Zehr, R. Stein, "What function do reflexes serve during human locomotion?", *Progress in Neurobiology*, vol. 58, pp. 185-205, 1999.
- [15] S. Rossignol, R. Dubuc, J.-P. Gossard, "Dynamic Sensorimotor Interactions in Locomotion", *Physiological Reviews*, vol. 86, pp. 89-154, 2006.
- [16] T. Luksch, K. Berns, "Initiating Normal Walking of a Dynamic Biped with a Biologically Motivated Control", *Proceedings of 11th International Conference on Climbing and Walking Robots (CLAWAR)*. Coimbra, Portugal, September 8-10 2008.
- [17] T. Luksch, K. Berns, "Controlling Dynamic Motions of Biped Robots with Reflexes and Motor Patterns", *Fourth International Symposium on Adaptive Motion of Animals and Machines (AMAM)*. Cleveland, USA, June 1-6 2008.
- [18] M. Proetzsch, T. Luksch, K. Berns, "Robotic Systems Design Using the Behavior-Based Control Architecture iB2C", to be published in *Journal of Robotics and Autonomous Systems*, 2009.
- [19] G. Pfaff, Ch. Meier, "Regelung elektrischer Antriebe II", third edition, Oldenbourg Verlag, 1992